

# Photochemical Deactivation Pathways of Microsolvated Hydroxylamine

Jittima Thisuwan<sup>a</sup>, Sermsiri Chaiwongwattana<sup>a,b,\*</sup>, Kritsana Sagarik<sup>a</sup> and

Nada Došlić<sup>b,\*</sup>

<sup>a</sup>*School of Chemistry, Institute of Science, Suranaree University of Technology,*

*Nakhon Ratchasima 30000, Thailand*

<sup>b</sup>*Ruđer Bošković Institute, 10000 Zagreb, Croatia*

\*E-mail:semsiri.chaiwongwattana@irb.hr, nadja.doslic@irb.hr

---

## Abstract

Hydroxylamine is a prototypical molecule displaying OH and NH bond interactions. Despite the early interest in the photolysis of NH<sub>2</sub>OH the primary mechanism of photodissociation remained unclear. Here we perform nonadiabatic trajectory-surface-hopping dynamics simulations based on the algebraic diagrammatic construction method to the second order (ADC(2)) and identify the dominant deactivation channel of NH<sub>2</sub>OH. By considering the photoinduced dynamics of hydroxylamine hydrates, ranging from monohydrates to tetrahydrates we show how this channel is modified by site specific addition of water.

---

## 1 Introduction

In the last two decades much effort has been devoted to the characterization of decay mechanisms of molecules which are constitutive subunits of

important biomolecular chromophores.<sup>1-4</sup> Prominent examples include chromophores such as pyrrole, imidazole or phenol, whose non-reactive decay is mediated by low-lying dissociative  $\pi\sigma^*$  states.<sup>5-10</sup> Interestingly, much less is known about the excited state dynamics of simpler chromophores such as hydroxylamine,  $\text{NH}_2\text{OH}$  whose photochemistry is dominated by Rydberg states.

Apart from being of considerable technological interest,<sup>11-13</sup> hydroxylamine is a prototypical example of a system displaying NH and OH bond interactions. In the context of fundamental molecular interactions between functional groups, the system has been intensively investigated in the ground electronic state.<sup>14-18</sup> Specifically, details of the intramolecular dynamics including: timescales of vibrational redistribution in high frequency stretching and bending motion, energy flow between the  $\text{NH}_2$  and OH moieties, and the mechanism of the torsion-inversion dynamics have been revealed by rovibrational spectroscopy.<sup>17,18</sup>

The dynamics of hydroxylamine in the excited electronic states has received less attention. The vacuum ultraviolet (VUV) absorption spectrum of hydroxylamine vapor in the range between 160 and 250 nm has been first reported by Betts and Back.<sup>19</sup> The same authors have investigated the photolysis of  $\text{NH}_2\text{OH}$  showing that  $\text{NH}_2 + \text{OH}$  and  $\text{NH}_2\text{O} + \text{H}$  are the primary processes of direct photolysis (Zn spectral lamp at 213 nm) with yields of 40% and 60%, respectively. On the other hand, mercury-sensitized decomposition of hydroxylamine yielded  $\text{NH}_3$  as a major product suggesting a primary decomposition into  $\text{NH}_2 + \text{OH}$ . More recently, Gericke et al. confirmed that the H atom channel dominates the photo fragmentation of hydroxylamine at 193 nm leads.<sup>20</sup> The quantum efficiency of the  $\text{NH}_2 + \text{OH}$  channel was found to be less than 0.10. The importance of H-atom formation at 193 nm was also confirmed by Crim and coworkers.<sup>21</sup> At 240 nm, however, NO bond dissociation became the main channel of hydroxylamine photodissociation. From the theoretical side, the authors have shown that the topography of the two lowest excited electronic

states, with initial excitation from the oxygen and the nitrogen lone pairs to a Rydberg orbital, dominate the photodissociation dynamics.<sup>21</sup> In aqueous solution, the stoichiometry of  $\text{NH}_2\text{OH}$  photolysis  $3\text{NH}_2\text{OH} \rightarrow \text{NH}_3 + 3\text{H}_2\text{O} + \text{N}_2$  and the detection of  $\text{NHOH}$  suggests  $\text{NH}_2 + \text{OH}$  as the primary photodissociation process.<sup>22</sup> However, considering the complexity of the mechanisms leading to the final stoichiometry alternative primary processes can be envisaged. Here these processes will be investigated.

This work presents results of a computational study directed toward understanding the mechanisms of excited state deactivation of hydroxylamine and of small hydroxylamine-water clusters,  $\text{NH}_2\text{OH}(\text{H}_2\text{O})_n$  with  $n = 1, 4$ . Understanding the role of water location and cluster size in the photofragmentation dynamics of hydroxylamine is important issue for acid-base chemistry as hydrogen bond formation may modify the ordering and character of the excited electronic states as well as the accessibility of the conical intersections. In addition, by increasing the size of the system interesting aspects of the competition between intrinsic relaxation of the chromophore, excited state proton transfer and redistribution of excess vibrational energy to the solvent can be studied in details.

## 2 Computational Methods

The initial ground state geometries of several of  $\text{NH}_2\text{OH}(\text{H}_2\text{O})_n$  clusters have been generated using the test particle model.<sup>23–25</sup> Subsequently the RI-MP2/aug-cc-pVDZ method has been used to optimize the ground state structures of these clusters and compute the Hessians which are needed for the generation of initial conditions in the dynamics simulations. Excited state computations were performed using the ADC(2) method<sup>26,27</sup> with the resolution of identity approximation (RI).<sup>28,29</sup> The aug-cc-pVDZ basis set has been used throughout the work.

ADC(2)-based nonadiabatic (NA) dynamics trajectory simulations have been performed by using an in-house software<sup>30–32</sup> based on Tully’s fewest switching surface hopping algorithm<sup>33,34</sup> with the decoherence correction of  $\alpha = 0.1E_h$ .<sup>35</sup> The program is interfaced to Turbomole 7.0.<sup>36</sup> Newton’s equations were integrated in time steps of  $\tau_1 = 0.5$  fs by using the velocity-Verlet algorithm, whereas the the time-dependent Schrödinger equation was integrated in steps of  $\tau_2 = 5 \times 10^{-5}$  fs.<sup>37</sup> The initial conditions were selected from the ground state,  $S_0$ , Wigner distribution<sup>38</sup> as explained in a recent work.<sup>32</sup> In order to simulate the photolysis of isolated hydroxylamine at 240 nm and 193 nm, NA trajectories have been started from the  $S_1$ , and  $S_1 - S_3$  states, respectively, and propagated in the manifold of the ground and four excited electronic states. All simulations of  $\text{NH}_2\text{OH}(\text{H}_2\text{O})_n$  clusters were initiated in the  $S_1$  state.

### 3 Results and Discussion

#### 3.1 Electronic structure calculations

In the ground electronic state the minimum energy geometry of  $\text{NH}_2\text{OH}$  is *trans* with  $C_s$  symmetry. Figure 1 displays the minimum energy structure of four hydroxylamine hydrates as optimized at the MP2/aug-cc-pVDZ level of theory. The relevant geometry parameters are collected in Table 1. The relative energies of several local minima and the corresponding structural parameters are given in Table S1. These are found significantly higher in energy and will not be considered further. Specifically in the monohydrates, the structure HW1-[2] (see Figure S1) in which the water molecule is H-bonded only to the hydroxyl group is found 2.06 kcal mol<sup>-1</sup> higher in energy. In going from HW1-[1] to HW4-[1] one notices the prolongation of the OH bond from 0.97 to 0.99 Å whereas the NO bonds remained virtually unaffected. Strengthening of the hydrogen bond with the closest water molecule can be followed also by

monitoring the OO distance which decreases from 2.85 Å in HW1-[1] to 2.73 Å in HW4-[1].

Basic excited state information is collected in Table 2. The vertical excitation energy of NH<sub>2</sub>OH to the  $S_1$  state of 6.25 eV (198 nm) finds very good agreement with the experimental absorption maximum at 193 nm. The  $S_1$  state is of *nRyd* character and corresponds to excitation from the lone pair orbitals on the O and N atoms to dominantly a 3s-like Rydberg orbital. In the hydrates, vertical excitations are in the range between 6.27 eV in HW3-[1] and 6.69 in HW4-[1]. The lowest *nRyd* state is predominantly a HOMO→LUMO transition with the HOMO localized on NH<sub>2</sub>OH. The frontier orbitals are shown in Figure 2 whereas the molecular orbitals involved in the four lowest singlet transitions are shown in Figures S2-S6. In going from HW1-[1] to HW4-[1] the transitions originating from excitation from the lone pair orbitals of the O atoms on the water molecules to delocalized Rydberg orbitals get stabilized. Specifically, the  $S_2$  state of HW4-[1], found only 0.26 eV above  $S_1$ , corresponds to such a state with implications for the dynamics that will be apparent soon.

Geometry optimization of NH<sub>2</sub>OH in the  $S_1$  state leads to OH bond dissociation. In the hydrates, the optimization promotes excited state proton transfer from NH<sub>2</sub>OH to water. From the geometries of the conical intersections one can see that the excess proton is located on water molecules that is not directly bound to NH<sub>2</sub>OH implying that a stepwise excited state proton transfer (ESPT) process takes place.

### 3.2 *Nonadiabatic dynamics simulations*

Let us start by considering the photoexcitation of NH<sub>2</sub>OH at the origin of the  $S_1$  transition, at 240 nm. A total of 127 trajectories has been launched from an energy window of  $240 \pm 2$  nm. We found OH bond dissociation to

be the dominant deactivation channel accounting for 83 % of the deactivation events. Deactivation *via* NO and NH bond dissociation was encountered in only 7 and 13 trajectories, respectively, while 2 trajectories yielded HNO+H<sub>2</sub>. The ultrafast deactivation of NH<sub>2</sub>OH by OH bond dissociation is an adiabatic process occurring on the  $S_1$  surface as evident from the trajectory displayed in Figure 3. During the dynamics the electron density is translocated from the lone pair orbitals to the Rydberg orbital that evolves into a  $\sigma^*$  orbital and the dissociation of the OH bond takes place. Note also that the energy of the ground state rises steeply within 10 fs, comparable to the OH vibrational period. The average population of the  $S_1$  state during the dynamics was fitted to an exponential time constant of only 28 fs. Due to the sub 50-fs time scale of OH dissociation, we believe that the primary process has not been captured in the experiments of Luckhaus *et al.*<sup>21</sup> Unfortunately the fate of the system after crossing to the ground state cannot be followed in our simulations. Being a single reference method ADC(2) is not suitable for simulating the dynamics at the  $S_1/S_0$  conical intersection.

The simulation of the dynamics after excitation at 193 nm, needs to account for the broad absorption spectrum of NH<sub>2</sub>OH. Therefore we have launched a total of 893 trajectories from the three lowest excited states. Initial conditions for the dynamics were selected by a weighted random algorithm according to the oscillator strengths of the transitions that fit the selected energy window.<sup>32</sup> Again, OH bond dissociation was found to be the dominant photochemical mechanism of relaxation in all three states accounting for 81%, 50% and 55% of the deactivation events in the  $S_1$ ,  $S_2$  and  $S_3$  states, respectively. NO bond dissociation is almost negligible (9%) when the system is initially excited to the  $S_1$  state, but becomes more important in the  $S_2$  and  $S_3$  states where it accounts for 29% and 23% of all deactivations. Further, simulations have revealed a small fraction of trajectories deactivating *via* NH bond dissociation mostly from the  $S_2$  states (12%). A characteristic nonadiabatic trajectory deactivating

by NO bond dissociation is shown in Figure 4. The dynamics is initiated in the  $S_1$  and the initial excitation is of  $nRyd$  character. The deactivation to the ground state involves two nonadiabatic transition at approximately 45 and 65 fs. The second nonadiabatic transition changes the character of the  $S_1$  state leading to NO bond dissociation.

To investigate the impact of water on the fragmentation dynamics of  $NH_2OH$  we performed NA dynamics simulation for the four lowest energy clusters displayed in Figure 1. On the basis of relative energies of ground state species (see Tables S1-S4) it is evident that with exception of HW4-[2], the Boltzmann population of the other clusters is negligible.

The results of the simulations, i.e., fragmentation channels of the hydrates, are compared in Table 3. In case of HW1-[1] a total of 176 trajectories were launched from the  $S_1$  state. It was found that OH bond breaking is the dominant deactivation mechanism accounting for 47% of the deactivation events, but a substantial fraction of trajectories (25 %) deactivated by ESPT yielding  $H_3O^+$ . Lifetimes of 50 fs and 36 fs were computed for the OH fission and ESPT mechanisms, respectively. Note that the former mechanism requires the *trans* to *cis* conversion of the  $NH_2OH$  moiety within HW1-[1] and the corresponding lifetime is longer than for isolated  $NH_2OH$ .

In going from the monohydrate to the tetrahydrate one sees the appearance of new deactivation mechanisms. Specifically, ESPT to water is the dominant deactivation channel in HW2-[1] and HW3-[1], while OH bond breaking on distal water molecules dominates the deactivation of HW4-[1]. It is interesting to note that in a number of cases the conical intersection with the ground state is reached after a stepwise proton transfer including two and even three water molecules. Figure S7 displays a characteristic HW3-[1] trajectory exhibiting stepwise ESPT.

Focusing on HW4-[1], Figure 5 shows a selected nonadiabatic trajectory deac-

tivating *via* dissociation of the free OH bond on a water molecule. The system is initially excited to the  $S_1$  state of  $nRyd$  character with excitation from the  $2p$  lone pair orbitals on the O and N atoms of  $NH_2OH$  to a diffuse  $3s$ -like Rydberg orbital. However as the energy gap between the  $S_1$  and  $S_2$  surfaces is very small the coupling between the two states leads to the change of the character of the  $S_1$  state within few fs. The state involves a translocation of electron density from the  $2p$  lone pair orbital of the O atom of a water to the Rydberg orbital. The migration of charge leads to elongation of the free OH bond on the water which leads to a strong destabilization of the ground electronic state. One can also see the subsequent change of the Rydberg orbital into a  $\sigma^*$  with electronic excitation localized along the OH bond.

Altogether, from the above results it is apparent that the photochemical pathways of  $NH_2OH$  deactivation are strongly influenced by the complexation with water. The effect of bulk water polarity on the ordering of the excited states and deactivation dynamics of  $NH_2OH$  has not been considered and calls for NA dynamics simulations in the framework of quantum-mechanics/molecular-mechanics (QM/MM) simulations. However, clear trends emerged already by considering a limited number of water molecules surrounding the chromophore.

## Summary

In this work we have shown that the primary processes of  $NH_2OH$  photolysis, both at 240 nm and 193 nm, corresponds to OH bond dissociation. The dissociation of the NO bond observed in early experiments as the dominant dissociation channel, is found to be a minor channel. In our opinion the sub-50 fs time scale of OH fission prevented the observation of the primary process. It can be envisaged that, upon relaxation to the ground electronic state, re-ollision with the parent ion can occur leading to NO bond dissociation on the longer time scale.

Further, we have shown how complexation with water strongly influences the photodissociation pathways of  $\text{NH}_2\text{OH}$ . From the one side direct and step-wise ESPT to water molecules is promoted. On the other side, the presence of water alters the ordering of the electronic states. Translocation of electron density from both, lone pair orbitals of  $\text{NH}_2\text{OH}$  and water, to Rydberg orbitals gives rise to electronic states separated by less than 0.5 eV. The strong coupling between these states determines the photodynamics. Consequently, in the tetrahydrate HW4-[1] splitting of water is found to be the dominant deactivation channel.

## Acknowledgment

The authors acknowledge support of the Croatian Science Foundation (no. 8238) and the financial supports provided by Suranaree University of Technology (SUT) through the SUT-Ph.D. program (SUT-Ph.D./05/2554). Dr. Sermsiri Chaiwongwattana received SUT post-doctoral research fellowship from Suranaree University of Technology and was supported by the Unity Through Knowledge Fund (UKF B1). Computer time was provided by the Croatian National Grid Infrastructure (CRONGI) and the high-performance computer facilities of the Suranaree University of Technology (SUT).

## References

- [1] A. L. Sobolewski, W. Domcke, *Chem. Phys.* 259 (2000) 181–191.
- [2] A. L. Sobolewski, W. Domcke, C. Dedonder-Lardeux, C. Jouvet, *Physical Chemistry Chemical Physics* 4 (7) (2002) 1093–1100.
- [3] C. E. Crespo-Hernández, B. Cohen, B. Kohler, *Nature* 436 (2005) 1141–1144.

- [4] A. L. Sobolewski, W. Domcke, Efficient Excited-State Deactivation in Organic Chromophores and Biologically Relevant Molecules: Role of Electron and Proton Transfer Processes, in: W. Domcke, D. Yarkony, H. Köppel (Eds.), Conical Intersections: Theory, Computation and Experiment, World Scientific, Singapore, 2011, pp. 51–82.
- [5] M. Ashfold, B. Cronin, A. Devine, R. Dixon, M. Nix, *Science* 312 (2006) 1637–1640.
- [6] M. G. D. Nix, A. L. Devine, B. Cronin, R. N. Dixon, M. N. R. Ashfold, *J. Chem. Phys.* 125 (2006) 133318–133318.
- [7] A. L. Devine, B. Cronin, M. G. D. Nix, M. N. R. Ashfold, *J. Chem. Phys.* 125 (2006) 184302–184302.
- [8] B. Cronin, A. L. Devine, M. G. D. Nix, M. N. R. Ashfold, *Phys. Chem. Chem. Phys.* 8 (2006) 3440–3445.
- [9] G. M. Roberts, V. G. Stavros, *Chem. Sci.* 5 (5) (2014) 1698–1722.
- [10] G. Wu, S. P. Neville, O. Schalk, T. Sekikawa, M. N. R. Ashfold, G. A. Worth, A. Stolow, *J. Chem. Phys.* 142 (2014) 074302/1–12.
- [11] M. A. Mantegazza, G. Leofanti, G. Petrini, M. Padovan, A. Zecchina, S. Bordiga, *Stud. Surf. Sci. Catal* 82 (1994) 541–550.
- [12] L. Xu, J. Ding, Y. Yang, P. Wu, *J. Catal.* 309 (2014) 1–10.
- [13] Z. Li et al., *Chem. Commun.* 51 (2015) 1930–1932.
- [14] S. Tsunekawa, *J. Phys. Soc. Jpn.* 33 (1972) 167–174.
- [15] F. G. Riddell, E. S. Turner, D. W. H. Rankin, M. R. Todd, *J. Chem. Soc. Chem. Commun.* 1979 (1979) 72–73.
- [16] D. W. H. Rankin, M. R. Todd, F. G. Riddell, E. S. Turner, *J. Mol. Struct.* 71 (1981) 171–183.
- [17] D. Luckhaus, *J. Chem. Phys.* 106 (1997) 8409–8426.

- [18] D. Luckhaus, Ber. Bunsenges. Phys. Chem. 101 (1997) 346–355.
- [19] J. Betts, R. A. Back, Can. J. Chem. 43 (1965) 2678–2684.
- [20] K.-H. Gericke, M. Lock, F. Schmidt, F. J. Comes, J. Chem. Phys. 101 (1994) 1988–1995.
- [21] D. Luckhaus, J. L. Scott, F. F. Crim, J. Chem. Phys. 110 (1999) 1533–1541.
- [22] D. Behar, D. Shapira, A. Treini, J. Phys. Chem. 76 (1972) 180–186.
- [23] K. Sagarik, R. Ahlrichs, J. Chem. Phys 81 (1987) 5117–5126.
- [24] K. Sagarik, J. Mol. Struct. (Theochem.) 465 (1999) 141–155.
- [25] K. Sagarik, S. Chaiwongwattana, P. Sisot, Chem. Phys 306 (2004) 1–12.
- [26] J. Schirmer, Phys. Rev. A 26 (1982) 2395–2416.
- [27] A. B. Trofimov, J. Schirmer, Chem. Phys. 214 (1997) 153–170.
- [28] C. Hättig, F. Weigend, J. Chem. Phys. 113 (2000) 5154–5161.
- [29] C. Hättig, A. Hellweg, A. Köhn, Phys. Chem. Chem. Phys. 8 (2006) 1159–1169.
- [30] J. Novak, M. Mališ, A. Prlj, I. Ljubić, O. Kühn, N. Došlić, J. Phys. Chem. A 116 (2012) 11467–11475.
- [31] D. Tuna, N. Došlić, M. Mališ, A. L. Sobolewski, W. Domcke, J. Phys. Chem. B 119 (2015) 2112–2124.
- [32] M. Sapunar, A. Ponzi, S. Chaiwongwattana, M. Mališ, A. Prlj, P. Decleva, N. Došlić, Phys. Chem. Chem. Phys. 17 (2015) 19012–19020.
- [33] J. C. Tully, J. Chem. Phys. 93 (1990) 1061–1071.
- [34] B. F. E. Curchod, U. Rothlisberger, I. Tavernelli, ChemPhysChem 14 (2013) 1314–1340.
- [35] G. Granucci, M. Persico, Critical appraisal of the fewest switches algorithm for surface hopping , J. Chem. Phys. 126 (2007) 134114/1–11.

- [36] TURBOMOLE V7.0 2015, a development of University of Karlsruhe and Forschungszentrum Karlsruhe GmbH, 1989-2007, TURBOMOLE GmbH, since 2007, available from <http://www.turbomole.com>.
- [37] L. Shampine, M. Gordon, Computer Solution of Ordinary Differential Equations: The Initial Value Problem, Freeman, 1975.
- [38] J. Tannor, David, Introduction to quantum mechanics: a time-dependent perspective, University Science Books, Sausalito, CA, 2007.

Table 1

Structural parameters of the lowest energy forms of  $\text{NH}_2\text{OH}(\text{H}_2\text{O})_n$  with  $n = 1, 4$  as optimized using the RI-MP(2)/aug-cc-pVDZ method. Distances in Å. The asymmetric stretching coordinate  $\Delta d_{DA}$  is the difference between the donor and acceptor OH bond. Relative energies and structural parameters of local minimum energy structures are given in Table S1.

System	H-bond	$R_{NO}^H$	$R_{OH}^H$	$R_{OO}$	$R_{NO}^W$	$\Delta d_{DA}$
HW1-[1]	(1)	1.45	0.97	2.85	-	1.07
	(2)			-	2.79	1.00
HW2-[1]	(1)	1.44	0.98	2.78	-	0.83
	(2)			-	2.83	0.87
	(3)			2.74	-	0.84
HW3-[1]	(1)	1.44	0.98	2.74	-	0.78
	(2)			-	2.82	0.84
	(3)			2.74	-	0.80
	(4)			2.73	-	0.77
HW4-[1]	(1)	1.44	0.99	2.73	-	0.76
	(2)			-	3.01	0.97
	(3)			-	2.81	0.81
	(4)			2.76	-	0.84
	(5)			2.75	-	0.80
	(6)			2.72	-	0.82

Table 2

ADC(2)/aug-cc-pVDZ vertical excitation energies (in eV), molecular orbitals involved in the lowest four singlet transitions and oscillator strengths ( $f$ ).

System	$E^{vert}$	Character	$f$
HW	6.25	H $\rightarrow$ L	0.018
	6.67	H-1 $\rightarrow$ L	0.008
	6.79	H $\rightarrow$ L+1	0.021
	7.24	H-1 $\rightarrow$ L+1	0.014
HW1-[1]	6.46	H $\rightarrow$ L	0.024
	6.84	H-1 $\rightarrow$ L	0.001
	7.14	H-2 $\rightarrow$ L	0.048
	7.29	H $\rightarrow$ L+3	0.025
HW2-[1]	6.35	H $\rightarrow$ L	0.023
	6.61	H-1 $\rightarrow$ L	$4 \cdot 10^{-4}$
	7.18	H $\rightarrow$ L+1	0.031
	7.26	H-2 $\rightarrow$ L	0.047
HW3-[1]	6.27	H $\rightarrow$ L	0.018
	6.65	H-1 $\rightarrow$ L	0.006
	7.06	H $\rightarrow$ L+1	0.017
	7.25	H-2 $\rightarrow$ L	0.034
HW4-[1]	6.69	H $\rightarrow$ L	0.019
	7.07	H-1 $\rightarrow$ L	0.039
	7.11	H $\rightarrow$ L+2	0.007
	7.20	H-2 $\rightarrow$ L	0.058

Table 3

Fragmentation channels of the hydroxylamine-water clusters,  $\text{NH}_2\text{OH}(\text{H}_2\text{O})_n$  with  $n=1,4$  as obtained from nonadiabatic dynamics simulations.

Mechanism	HW1-[1]	HW2-[1]	HW3-[1]	HW4-[1]
OH	47	14	-	4
ESPT	25	51	41	32
NH	11	8	8	-
W(OH)	10	9	16	40
NO	8	11	16	6
other	7	7	19	17

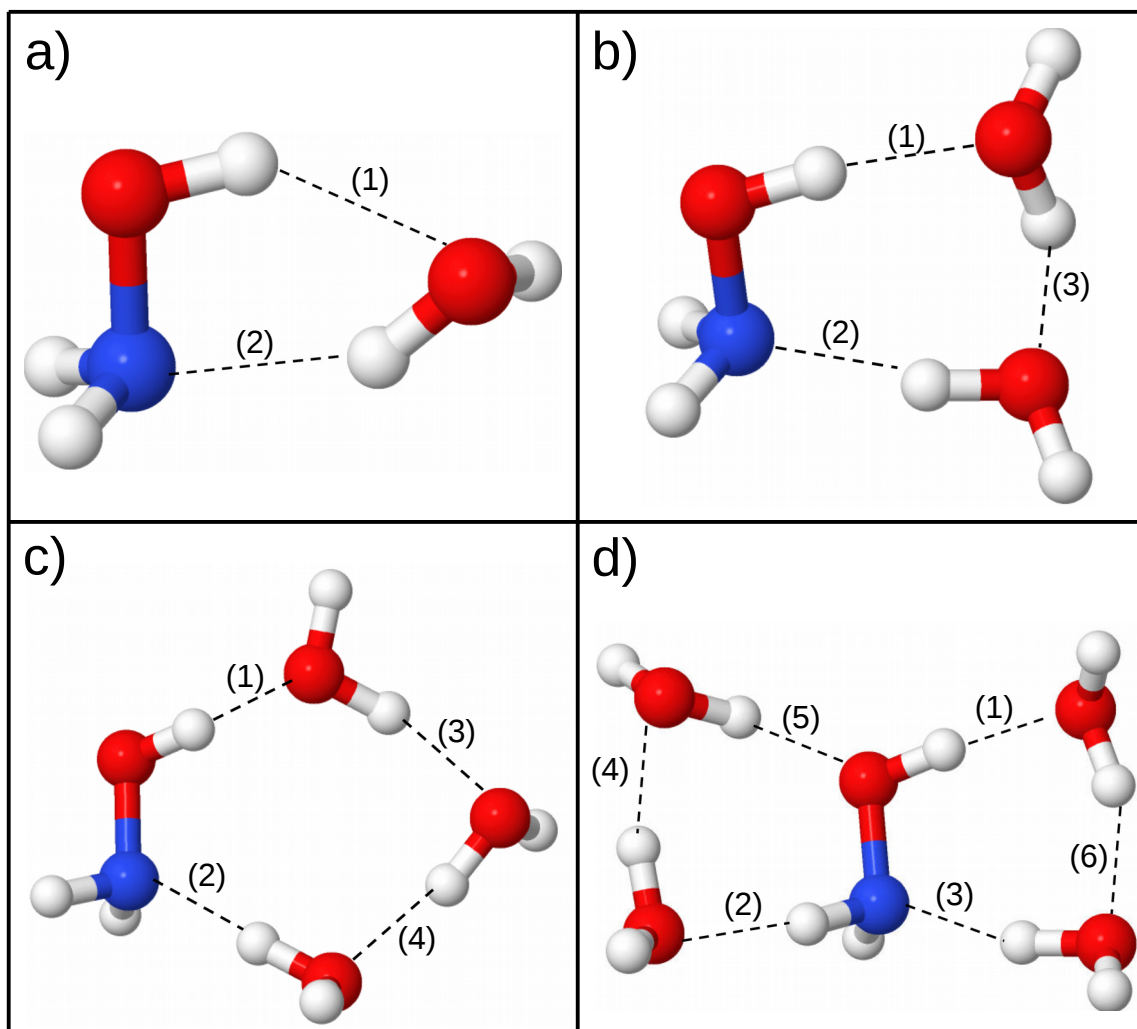


Fig. 1. Minimum energy structures of  $\text{NH}_2\text{OH}(\text{H}_2\text{O})_n$  with  $n = 1, 4$  as optimized using the RI-MP(2)/aug-cc-pVDZ method. Top a) HW1-[1], b) HW2-[1], bottom c) HW3-[1] and d) HW4-[1]. The numeration of hydrogen bonds (1) -(6) is given to facilitate to comparison of the structural parameters given in Table 1.

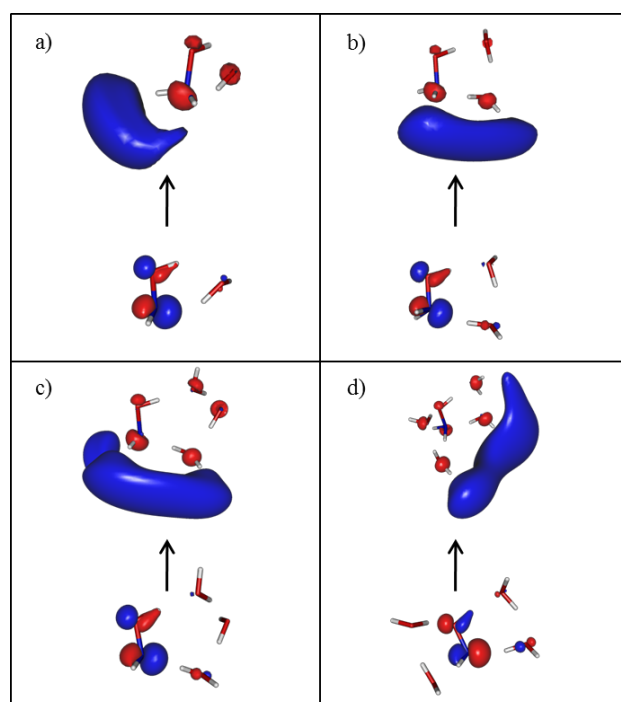


Fig. 2. Frontier molecular orbitals involved in the  $S_1$  transition at the geometry of vertical excitation. Top a) HW1-[1], b) HW2-[1], bottom c) HW3-[1] and d) HW4-[1]. Computation performed at the ADC(2)/aug-cc-pVDZ level.

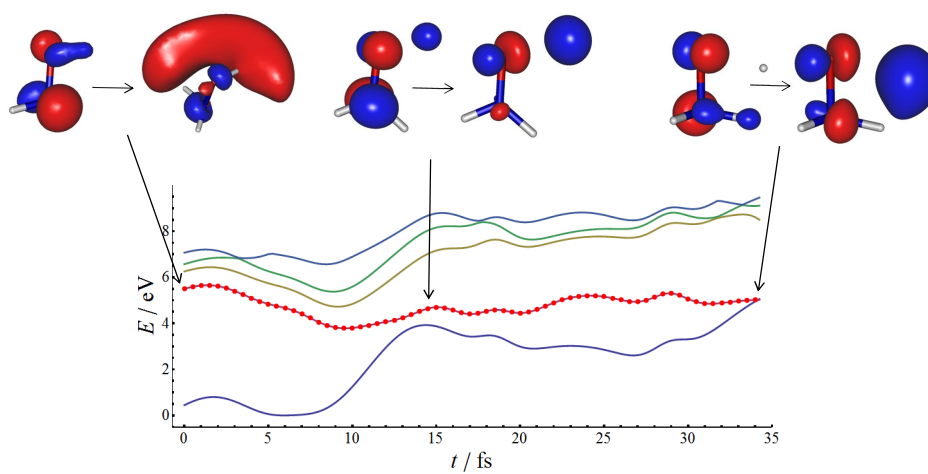


Fig. 3. Energies of the electronic states along a selected non-adiabatic trajectory of  $\text{NH}_2\text{OH}$  computed at the ADC(2)/aug-cc-pVDZ level. After excitation at 240 nm the deactivation to  $S_0$  occurs by OH bond dissociation. The electronic state in which the trajectory resides is marked with red dots. The insets show the leading excitations contributing to  $S_1$ .

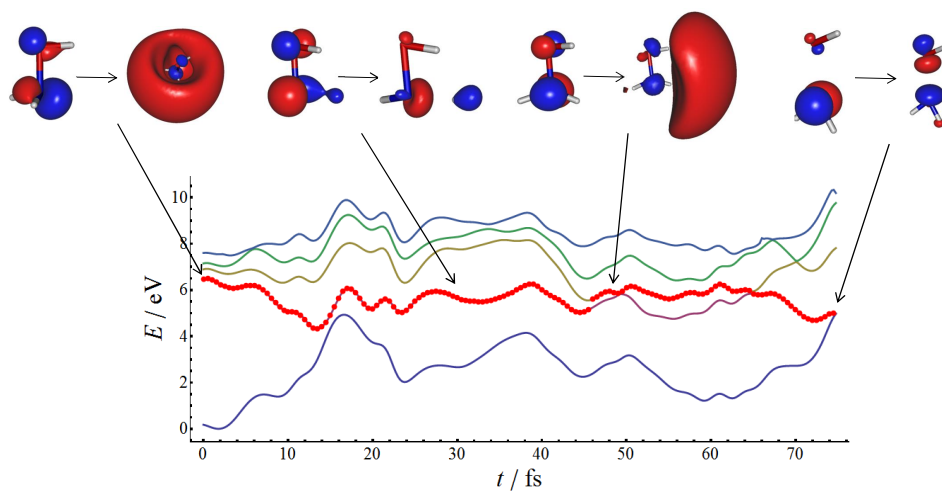


Fig. 4. Energies of the electronic states along a selected non-adiabatic trajectory of  $\text{NH}_2\text{OH}$  computed at the ADC(2)/aug-cc-pVDZ level. After excitation at 240 nm deactivation to  $S_0$  occurs by NO bond dissociation. The electronic state in which the trajectory resides is marked with red dots. The insets show the leading excitations contributing to  $S_1$ . The nonadiabatic transition at 65 fs leads to NO bond dissociation.

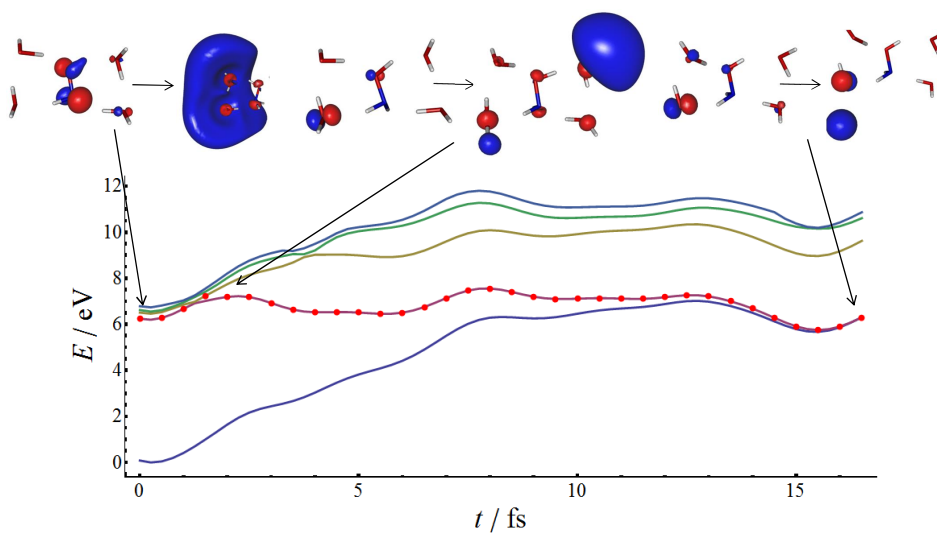


Fig. 5. Selected non-adiabatic trajectory of HW4-[1]. Deactivation to  $S_0$  occurs by dissociation of a free OH bond of a water molecule. The insets show the leading excitations contributing to  $S_1$ .

## Highlights

- For the first time the excited electronic states of hydroxylamine and hydroxylamine-water clusters with 1-4 water molecules are investigated at the ADC(2) level.
- First nonadiabatic dynamics study of hydroxylamine and hydroxylamine-water clusters
- OH bond dissociation is the primary process in  $\text{NH}_2\text{OH}$  photolysis.
- Complexation with water suppresses the primary process.
- In the hydrates excited state proton transfer is the main deactivation pathway.

Dear Editor,

On behalf of the authors, I would like to submit the manuscript entitled "Photochemical Deactivation Pathways of Microsolvated Hydroxylamine" to be considered for publication in Journal of Photochemistry and Photobiology A: Chemistry

Hydroxylamine is the smallest system displaying NH and OH bond interactions. The last investigation of hydroxylamine dates from 1999, whereas the hydrates were never investigated. In this contribution, we investigated the photodynamics of hydroxylamine taking place upon excitation in the wavelength range of 240 – 193 nm as well as the photodynamics of hydroxylamine-water clusters. We used non-adiabatic dynamics simulations based on the algebraic diagrammatic construction method to the second order (ADC(2)) for electronic structure determination to provide an accurate description of the state-specific deactivation.

Taking into account that hydroxylamine is also of considerable technological interest we believe that our results are important and of interest to the readers of Journal of Photochemistry and Photobiology A.

We look forward to hearing from you.  
Sincerely.

Dr. Nađa Došlić  
Senior scientist  
Department of Physical Chemistry,  
R. Bošković Institute  
Zagreb, Croatia  
E-Mail: nadja.doslic@irb.hr

**File(s) excluded from PDF**

The following file(s) will not be converted:

nh2oh.tex

Please click 'Download zip file' to download the most recent files related to this submission.